Behavioral/Systems/Cognitive

Gamma-Band Oscillations in the Primary Somatosensory Cortex—A Direct and Obligatory Correlate of Subjective Pain Intensity

Z. G. Zhang,[1,2]* L. Hu,[3]* Y. S. Hung,[2] A. Mouraux,[4] and G. D. Iannetti[1]

[1]Department of Neuroscience, Physiology and Pharmacology, University College London, London WC1E 6BT, United Kingdom, [2]Department of Electrical and Electronic Engineering, The University of Hong Kong, Hong Kong, China, [3]Key Laboratory of Cognition and Personality (Ministry of Education) and School of Psychology, Southwest University, Chongqing 400715, China, and [4]Institute of Neurosciences (IoNS), Université catholique de Louvain, Brussels B-1200, Belgium

Electroencephalographic gamma band oscillations (GBOs) induced over the human primary somatosensory cortex (SI) by nociceptive stimuli have been hypothesized to reflect cortical processing involved directly in pain perception, because their magnitude correlates with pain intensity. However, as stimuli perceived as more painful are also more salient, an alternative interpretation of this correlation is that GBOs reflect unspecific stimulus-triggered attentional processing. In fact, this is suggested by recent observations that other features of the electroencephalographic (EEG) response correlate with pain perception when stimuli are presented in isolation, but not when their saliency is reduced by repetition. Here, by delivering trains of three nociceptive stimuli at a constant 1 s interval, and using different energies to elicit graded pain intensities, we demonstrate that GBOs recorded over SI always predict the subjective pain intensity, even when saliency is reduced by repetition. These results provide evidence for a close relationship between GBOs and the cortical activity subserving pain perception.

Introduction

Stimulus-induced enhancements of electroencephalographic (EEG) power in the gamma frequency range (30–100 Hz) have been consistently observed in multiple sensory modalities (Womelsdorf et al., 2006; Fries, 2009; Karns and Knight, 2009; Herrmann and Kaiser, 2011) and hypothesized to play a crucial role in cortical integration and perception (Tallon-Baudry et al., 1997; Rodriguez et al., 1999). Recently, using electroencephalography and magnetoencephalography (MEG), it has been reported that also nociceptive stimuli elicit gamma-band oscillations (GBOs) within the human primary somatosensory cortex (SI; Gross et al., 2007; Hauck et al., 2007). Because the magnitude of these GBOs correlates with the subjective pain intensity, it has been suggested that they reflect cortical activity related directly to the perception of pain (Gross et al., 2007; Schulz et al., 2011b).

Received Nov. 24, 2011; revised Feb. 9, 2012; accepted Feb. 23, 2012.

Author contributions: A.M. and G.D.I. designed research; Z.G.Z., L.H., Y.S.H., A.M., and G.D.I. performed research; Z.G.Z., L.H., and Y.S.H. analyzed data; Z.G.Z., L.H., A.M., and G.D.I. wrote the paper.

Z.G.Z. and Y.S.H. acknowledge the support of the Hong Kong SAR Research Grants Council (HKU762111M). L.H. is supported by the Fundamental Research Funds for the Central Universities (SWU1109010) and Doctoral Foundation of Southwest University (SWU111079).

G.D.I. is University Research Fellow of The Royal Society, and acknowledges the support of the Biotechnology and Biological Sciences Research Council.

*Z.G.Z. and L.H. contributed equally to this work.

The authors declare no competing financial interests.

Correspondence should be addressed to Dr. Giandomenico Iannetti, Department of Neuroscience, Physiology and Pharmacology, University College London, Medical Sciences Building, Gower Street, WC1E 6BT London, UK. E-mail: g.iannetti@ucl.ac.uk.

DOI:10.1523/JNEUROSCI.5877-11.2012

 0270-6474/12/327429-10$15.00/0

However, the described relationship between the magnitude of GBOs and pain perception (Gross et al., 2007) cannot, as such, be considered as evidence that GBOs are related directly to the pain experience. Indeed, because these GBOs were elicited by transient and intense nociceptive stimuli presented in isolation, the observed relationship could also be interpreted as the indirect consequence of the fact that stimuli perceived as more painful are also necessarily more salient and, thus, more prone to trigger mechanisms of attentional capture or arousal (Iannetti and Mouraux, 2010; Legrain et al., 2011). In fact, this alternative interpretation has been recently shown to explain the well characterized relationship between the intensity of pain perception and the magnitude of virtually all other features of the nociceptive-evoked EEG response (e.g., the N1, N2, and P2 waves of laser-evoked potentials), thus suggesting that these responses reflect non-pain-specific processes related to attentional capture or arousal (Downar et al., 2000).

For these reasons, a crucial question must be addressed: are laser-induced GBOs truly and directly related to the intensity of pain perception (Gross et al., 2007; Schulz et al., 2011b)? Or, such as the other EEG responses to nociceptive stimuli, is their magnitude largely determined by stimulus saliency (Iannetti et al., 2008)?

Here we addressed this question using an experimental design consisting in the repetition of three identical nociceptive stimuli (1) at a short and constant 1 s interstimulus interval (ISI), to reduce the novelty of the repeated stimuli, and (2) using four different stimulus energies, to elicit graded intensities of pain perception. Using a point-by-point repeated-measures ANOVA combined with nonparametric permutation testing to compare

the time-frequency representations of the oscillatory EEG responses triggered by each of the three nociceptive stimuli repeated at a constant 1 s interval, we found that, unlike all other features of the nociceptive-evoked EEG response, the magnitude of GBOs correlates significantly with the intensity of pain perception, independently of stimulus repetition. This correlation was maximal over the scalp electrodes overlying the left and right SIs. Furthermore, using a Granger causality analysis, we observed that the GBOs recorded over the SI contralateral to the stimulated hand causally determine the GBOs recorded over the SI ipsilateral to the stimulated hand.

Together, our results show that, unlike all other well studied features of the EEG response to nociceptive input, GBOs predict the amount of pain perceived by a human participant, independently of the novelty content of the stimulus, thus indicating that GBOs could reflect cortical activity related directly to the emergence of painful percepts in humans.

Materials and Methods

Participants, experimental paradigm, and EEG recording

The analyses of this study were performed on the dataset collected for a previous study (Iannetti et al., 2008). Seven healthy subjects (five men and two women) aged 24–42 years (mean 29 ± 6) participated in the study. All participants gave written informed consent, and the local ethics committee approved the experimental procedures.

Participants were seated in a comfortable chair and wore protective goggles. They were asked to focus on the stimulus, relax their muscles and keep their eyes open while gazing slightly downward. Noxious radiant-heat stimuli were generated by an infrared neodymium yttrium aluminum perovskite laser with a wavelength of 1.34 μm (Electronical Engineering). These laser pulses activate directly and selectively nociceptive terminals located in the most superficial skin layers (Baumgärtner et al., 2005; Iannetti et al., 2006). Laser pulses were directed to the dorsum of the right and left hands, in two separate sessions performed on the same day. Data were collected from the right and left hands to (1) increase the total number of trials and, thereby, maximize the signal-to-noise ratio of the elicited EEG responses, and (2) determine whether the elicited EEG responses were lateralized as a function of the stimulated side. A coaxial He-Ne laser pointed to the area to be stimulated. The duration of the laser pulses was 4 ms. Beam diameter was set at ~7 mm (38 mm^2) by focusing lenses. Four different stimulus energies were used (E1: 2 J; E2: 2.5 J; E3: 3 J; E4: 3.5 J).

Stimuli were delivered in trains consisting of three consecutive stimuli (S1, S2, S3) of identical energy (E1, E2, E3, or E4), separated by a constant 1 s interstimulus interval. The time interval between two consecutive trains was 20 s. Three to six seconds after the end of each train, participants were asked to rate verbally the intensity of the pricking sensation elicited by each of the three laser stimuli, using a numerical rating scale ranging from 0 to 10, where 0 was defined as "no pain" and 10 was defined as "pain as bad as it can be" (Jensen and Karoly, 2001). In each session, 20 trains at each of the four energies (E1–E4) were delivered, in random order, for a total of 80 trains per session.

The electroencephalogram was recorded continuously using seven Ag-AgCl electrodes placed on the scalp according to the International 10–20 system (Fz, Cz, Pz, C3, C4, T3, and T4), using the nose as a common reference. To monitor ocular movements and eye blinks, electro-oculographic (EOG) signals were simultaneously recorded from two surface electrodes, one placed over the lower eyelid, the other placed 1 cm lateral to the outer corner of the orbit. Signals were amplified and digitized using a sampling rate of 4096 Hz and a precision of 12 bits, giving a resolution of 0.195 μV $digit^{-1}$ (System Plus; Micromed).

EEG data analysis

The EEG data were preprocessed using Letswave (Mouraux and Iannetti, 2008), a free signal-processing toolbox developed in Delphi 7.0, and EEGLAB (Delorme and Makeig, 2004), an open source toolbox running under the MATLAB (version 7.12, MathWorks) environment.

EEG data preprocessing. Continuous EEG data were bandpass filtered from 1 to 30 Hz (for analysis in the time domain) and from 1 to 100 Hz (for analysis in the time-frequency domain). EEG epochs were extracted using a window ranging from 1 s before the onset of the first stimulus (S1) to 1 s after the onset of the third stimulus (S3) of each train (total epoch duration: 4 s) and baseline corrected using the interval ranging from −1 to 0 s relative to the onset of S1.

Trials contaminated by eye-blinks and movements were corrected using an independent component analysis (ICA) algorithm (Makeig et al., 1997; Jung et al., 2001; Delorme and Makeig, 2004). In all datasets, individual eye movements, showing a large EOG channel contribution and a frontal scalp distribution, were clearly seen in the removed independent components. EEG epochs were then visually inspected and trials contaminated by artifacts due to gross movements were removed.

After artifacts rejection, EEG epochs were classified in four categories (I1–I4) according to the intensity of the painful percept elicited by the stimulus. This was achieved by rescaling the ratings of each participant between 0 and 100, defining 0 as the smallest pain rating and 100 as the largest pain rating of that participant (Iannetti et al., 2008). For each participant, trials were classified in four categories (I1: ≤25, I2: >25 and ≤50, I3: >50 and ≤75, I4: >75). Trials in each category were averaged together, thus obtaining four average waveforms for each participant. The average number of trials in each category (I1–I4) was not significantly different ($F = 0.38$, $p > 0.77$, one-way ANOVA).

Time-frequency analysis. A time-frequency representation of each single EEG epoch was obtained using a windowed Fourier transform (WFT) with a fixed 200 ms width Hanning window. Such a time-frequency analysis was chosen to achieve a good tradeoff between time resolution and frequency resolution in the range of gamma band EEG frequencies (30–100 Hz). In previous studies, laser-induced gamma-band oscillations have been observed at a latency of ~200 ms after stimulus onset, within a frequency range of 50 to 100 Hz (Gross et al., 2007; Tiemann et al., 2010). A 200 ms Hanning window is appropriate for identifying these responses, as (1) it provides a sufficiently high frequency resolution of 5 Hz, (2) it is adequate to avoid contamination of the estimates of post-stimulus EEG responses by prestimulus activity, (3) it is in line with the duration of GBOs described by Gross et al. (2007) and Schulz et al. (2011b).

The WFT yielded, for each single trial, a complex time-frequency spectral estimate $F(t, f)$ at each point (t, f) of the time-frequency plane extending from −1 to +3 s in the time domain, and from 1 to 100 Hz (in steps of 1 Hz) in the frequency domain. The magnitude of the stimulus-induced changes in oscillation amplitude (expressed as ER%) was estimated as follows:

$$ER\%(t, f) = [P(t, f) - R(f)]/R(f) \times 100 \quad (1)$$

where $P(t,f) = |F(t,f)|^2$ is the power spectral density at each time-frequency point (t, f), and $R(f)$ is the average power spectral density of the signal enclosed within the prestimulus reference interval (−900 to −100 ms before the onset of S1), for each estimated frequency f. The obtained time-frequency maps were then segmented into three separate maps ranging from 0 to 1 s relative to the onset of S1, S2, and S3, respectively. For each participant, condition (I1–I4) and stimulus (S1–S3), across-trial averaging of the ER% time-frequency representations yielded a time-frequency plot showing the average stimulus-induced changes of EEG oscillation power. Such time-frequency representations contain both phase-locked (laser-evoked potentials, LEPs) and non-phase-locked (event-related synchronization and desynchronization, ERS and ERD) EEG responses.

Furthermore, to distinguish between phase-locked and non-phase-locked EEG responses, the phase-locking value (PLV; Lachaux et al., 1999), which represents a measure of phase synchrony across trials, was calculated for each condition (I1–I4) and stimulus (S1–S3) of each participant, as follows:

$$PLV(t, f) = \left| \frac{1}{N} \sum_{n=1}^{N} \frac{F_n(t, f)}{|F_n(t, f)|} \right| \quad (2)$$

where N is the number of trials. The PLV values, used thereinafter, were baseline corrected using the prestimulus reference interval (−900 to −100 ms before the onset of S1) for each estimated frequency f.

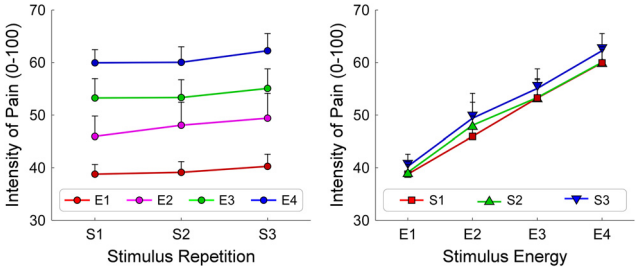

Figure 1. Relationship between stimulus energy, stimulus repetition, and intensity of pain. Radiant heat (neodymium yttrium aluminum perovskite or Nd:YAP laser) stimuli were delivered in triplets (S1–S3), using 4 stimulus energies (E1–E4) and constant ISI of 1 s. Error bars represent the SEM. The stimulus energy was identical across the 3 stimuli constituting the triplet. Left, *x*-axis, stimulus number; *y*-axis, rescaled intensity of pain. Right, *x*-axis, stimulus energy; *y*-axis, rescaled intensity of pain. Note that intensity of pain perception was significantly and positively correlated with the stimulus energy (E1–E4), but not affected by stimulus repetition (S1–S3).

Point-by-point time-frequency statistical analysis. A point-by-point two-way repeated-measures ANOVA, combined with nonparametric permutation testing (Maris and Oostenveld, 2007), was used to assess the effects of stimulus repetition (S1–S3) and intensity of pain perception (I1–I4) on the stimulus-induced modulations of EEG power (ER%), and to define the significant regions of interest (ROIs) within the time-frequency spectrograms obtained at each EEG channel. This was performed in the following five steps.

First, each point (t, f) of the ER% time-frequency maps was compared using a two-way repeated-measures ANOVA, with "stimulus repetition" (three levels: S1–S3) and "intensity of pain" (four levels: I1–I4) as factors. This yielded three time-frequency maps of *F*-values, representing (1) the main effect of stimulus repetition, (2) the main effect of intensity of pain and (3) the interaction between the two factors. Time-frequency points with a *p*-value ≤ 0.01 ($F \geq 4.44$ for the factor intensity of pain, $F \geq 5.72$ for the factor stimulus repetition, and $F \geq 5.07$ for their interaction) were selected for subsequent analyses.

Second, to account for the multiple-comparison problem in the point-by-point statistical analysis of time-frequency representations (Maris and Oostenveld, 2007), significant time-frequency points ($p \leq 0.01$) were categorized in clusters based on their adjacency in the time-frequency plane (cluster-level statistical analysis). Only clusters composed of >10 adjacent significant time-frequency points were considered, to account for the problem of multiple comparisons. The sum of the *F*-values of all time-frequency points composing a cluster, defined its cluster-level statistics (Σ_F).

Third, for every participant, we randomly permutated 5000 times the time-frequency representations of the 12 conditions ([S1 S2 S3]×[I1 I2 I3 I4]). In each permutation, the same two-way repeated-measures ANOVA was performed at every time-frequency point of the clusters identified in the second step, thus yielding a cluster-level statistics $\Sigma'_F(m)$ at the *m*-th permutation. Permutation distributions $D(\Sigma_F)$ of the cluster-level *F*-statistics were obtained from $\Sigma'_F(m)$.

Fourth, for each cluster identified in the second step, its two-tailed *p*-value p_F was obtained by locating the observed Σ_F under the permutation distribution $D(\Sigma_F)$ estimated from permutated $\Sigma_F(m)$.

Fifth, clusters were used to define time-frequency ROIs for the subsequent quantitative analysis based on two criteria: (1) the cluster had a *p*-value smaller than a defined threshold ($p_F \leq 0.01$); (2) only the cluster with the largest Σ_F in the high-frequency region ($\geq$30 Hz) and the cluster with the largest Σ_F in the low-frequency region ($<$30 Hz) were selected to control for false-positive observations (Maris and Oostenveld, 2007). Thereby, within the entire time-frequency plane obtained at a given EEG channel, significant clusters were used to define up to two time-frequency ROIs (one below and one above 30 Hz) characterizing the main effect of stimulus repetition, the main effect of intensity of pain and the interaction between the two factors.

Last, the same statistical analysis (point-by-point, two-way repeated-measures ANOVA and nonparametric permutation testing) was performed to investigate the effect of the experimental factors stimulus repetition (three levels: S1–S3) and "stimulus energy" (four levels: E1–E4), on the time-frequency representations of power magnitude (ER%).

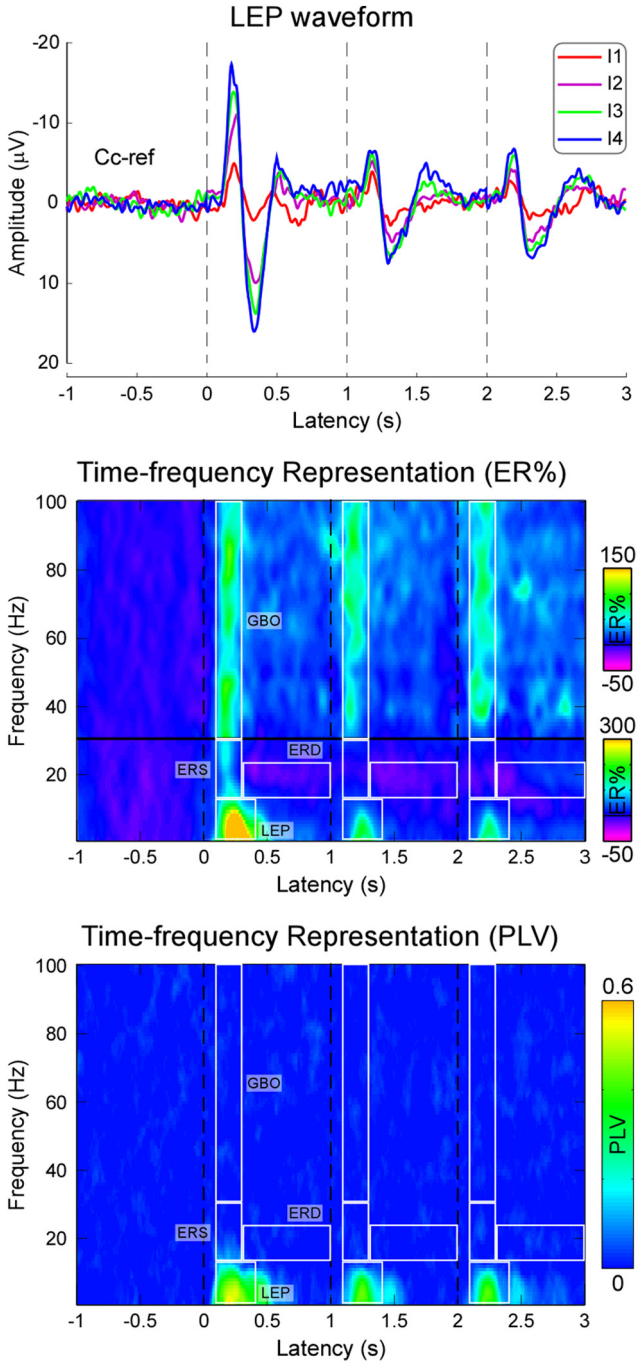

Figure 2. Group-level average ERPs elicited by laser stimuli (S1, S2, and S3). The vertical dashed lines mark the onset of the three laser stimuli (S1–S3). Displayed signals were recorded at electrode Cc (nose reference). Top, Group-level average LEPs at different intensity of pain (I1–I4) in the time domain. *x*-axis, time (s); *y*-axis, magnitude (μV). Middle, Group-level average time-frequency representation of laser-elicited modulation of EEG oscillation magnitude (ER%). *x*-axis, time (s); *y*-axis, frequency (Hz). The color scale represents the average increase (ERS%) or decrease (ERD%) of oscillation magnitude, relative to a prestimulus reference interval (−0.9 to −0.1 s before the onset of S1). Bottom, Group-level average PLV of laser-evoked brain responses. *x*-axis, time (s); *y*-axis, frequency (Hz). The color scale represents the average increase of PLV to the onset of the stimulus, relative to a prestimulus reference interval (−0.9 to −0.1 s before the onset of S1).

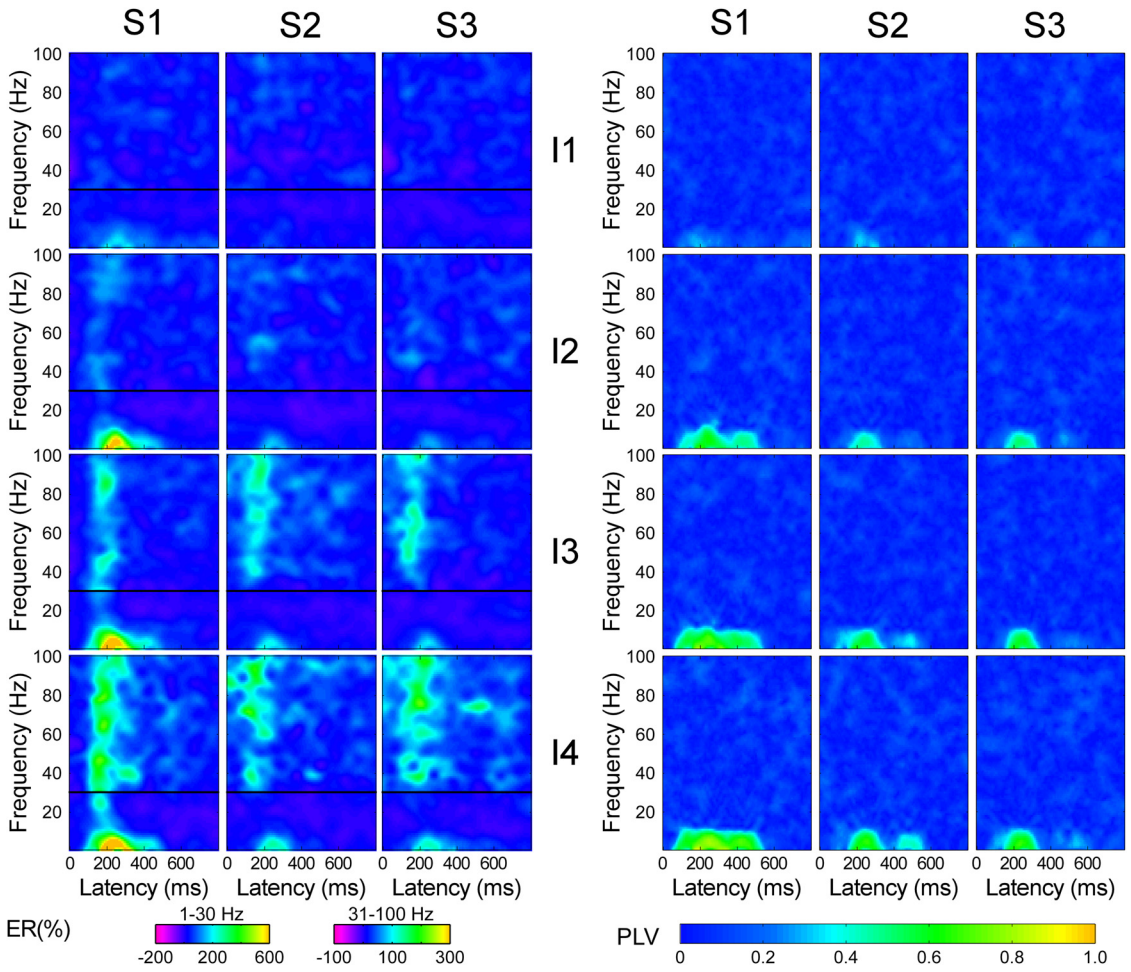

Figure 3. Time-frequency representations (ER% and PLV) of laser-EEG responses elicited by S1, S2, and S3, and at different intensity of pain (I1–I4). Displayed signals were recorded at electrode Cc (nose reference). EEG epochs were classified in 12 (3 × 4) categories according to the stimulus repetition (S1, S2, and S3) and the rescaled intensity of pain (I1, 0–25; I2, 26–50; I3, 51–75; and I4, 76–100). *x*-axis, time (ms); *y*-axis, frequency (Hz). Left, Time-frequency representations of laser-induced modulation of EEG oscillation magnitude (ER%) in 12 categories. The color scale represents the average increase (ERS%) or decrease (ERD%) of oscillation magnitude, relative to a prestimulus reference interval (−0.9 to −0.1 s before the onset of S1). Right, PLV of laser-evoked brain responses in 12 categories. The color scale represents the average increase of PLV to the onset of the stimulus, relative to a prestimulus reference interval (−0.9 to −0.1 s before the onset of S1).

Region-of-interest statistical analysis. As the point-by-point statistical analysis of the time-frequency maps obtained at each scalp electrode showed that stimulus-induced GBOs were maximal at the central electrode contralateral to the stimulated hand (Cc: C3 and C4 for right and left hand stimulation, respectively), and as previous studies have also shown such a scalp distribution (Gross et al., 2007; Hauck et al., 2007; Tiemann et al., 2010), the Cc electrode was selected to compute summary values for each significant time-frequency ROI of each participant, as follows. We first computed the mean of all time-frequency points within that ROI for each participant, stimulus (S1–S3) and intensity of pain perception (I1–I4). The obtained summary values were then compared using a two-way repeated-measures ANOVA, with stimulus repetition (S1–S3) and intensity of pain (I1–I4) as factors. When the effect of stimulus repetition was significant, we performed a *post hoc* analysis using a paired-sample *t* test to compare the responses elicited by S1, S2, and S3. When the effect of intensity of pain was significant, we performed (1) a *post hoc* analysis using a paired-sample *t* test to compare the responses related to I1, I2, I3, and I4 and (2) a *post hoc* analysis using a linear regression between intensity of pain perception and response magnitude. When the interaction between the two factors was significant, we performed a *post hoc* analysis comparing the slopes of the linear regression between intensity of pain perception and response magnitude for S1, S2, and S3, to assess how the correlation between intensity of pain and response magnitude was affected by stimulus repetition.

The same procedure was used to assess the effect of the factors stimulus repetition (S1–S3) and stimulus energy (E1–E4), thus exploring possible different effects of subjective pain intensity (I1–I4) and stimulus energy (E1–E4) on the time-frequency representations of laser-induced EEG oscillations.

Granger causality analysis. To reveal the causal relationship between the peaks of activity detected at the central electrodes contralateral and ipsilateral to the stimulated hand, we calculated the Granger causality index (Granger, 1969) between the neural activities sampled at Cc and at Ci. The Granger causality has been recently demonstrated to be a powerful and effective tool for evaluating both the direction and the strength of the causality between different neuronal activations (Astolfi et al., 2007; Ploner et al., 2009; Sato et al., 2009; Schoffelen and Gross, 2009). The dynamics of the neural responses at Cc (x_c) and Ci (x_i) can be described using a bivariate linear autoregressive model as:

$$x_c(t) = \sum_{j=1}^{P} a_j^{(cc)} x_c(t-j) + \sum_{j=1}^{P} a_j^{(ic)} x_i(t-j) + e_c(t) \quad (3)$$

$$x_i(t) = \sum_{j=1}^{P} a_j^{(ci)} x_c(t-j) + \sum_{j=1}^{P} a_j^{(ii)} x_i(t-j) + e_i(t) \quad (4)$$

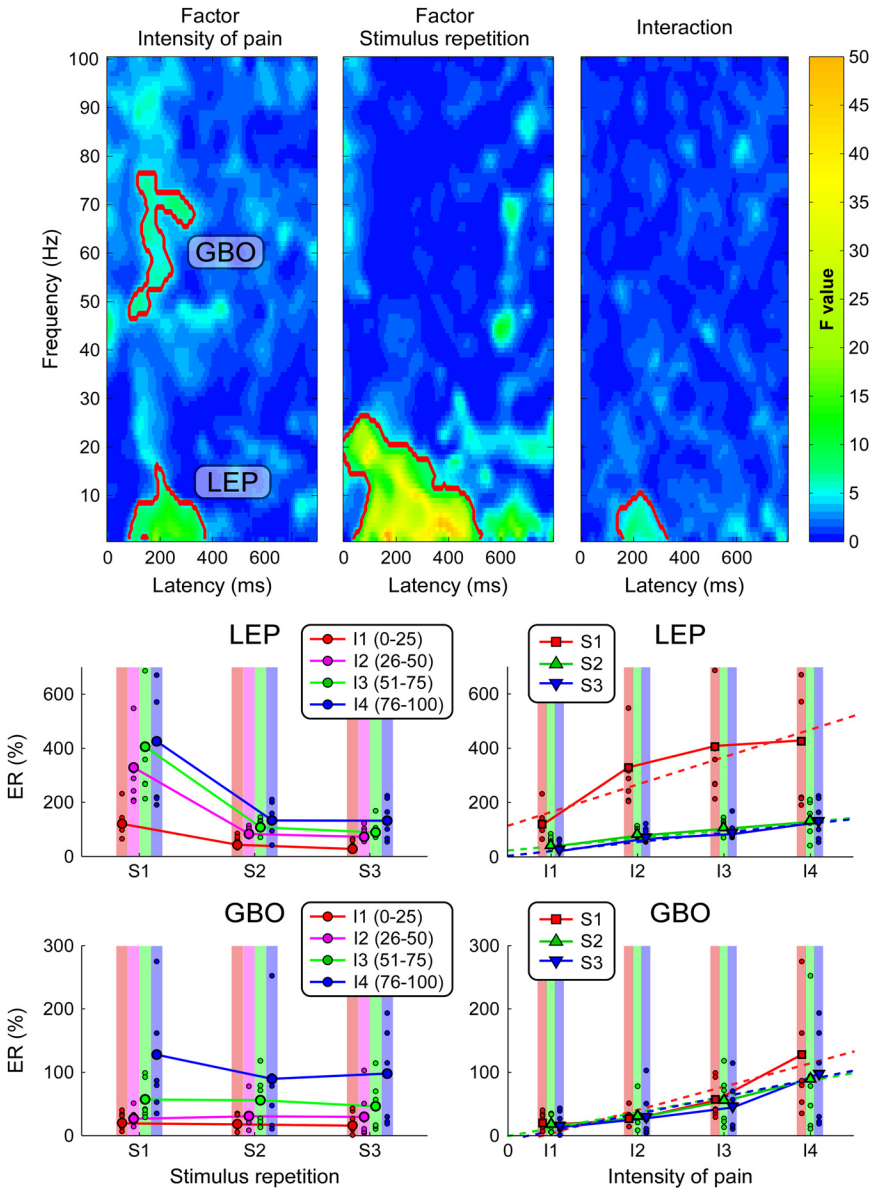

Figure 4. Effect of stimulus repetition (S1–S3) and intensity of pain (I1–I4) on the time-frequency representations of laser-induced modulation of EEG oscillation magnitude (ER%). Top, Two-way repeated-measures ANOVA to assess the effect of stimulus repetition and intensity of pain on the time-frequency representations of LEPs (ER%) and nonparametric permutation testing (Maris and Oostenveld, 2007) to define regions of interest. *x*-axis, time (ms); *y*-axis, frequency (Hz). The time-frequency pixels significantly affected by each experimental factor (or by the interaction between the two factors) are outlined in red. The color scale represents the *F*-values for each of the factors and their interaction. Note that the time-frequency points with $p < 0.01$ ($F > 4.44$ for the factor intensity of pain; $F > 5.72$ for the factor stimulus repetition, and $F > 5.07$ for their interaction) were selected for the subsequent nonparametric permutation testing. The factor intensity of pain significantly modulated the time-frequency representations in two distinct regions (in red): low-frequency cluster (LEP: 86–367 ms, 1–16 Hz) and high-frequency gamma band cluster (GBO: 86–328 ms, 47–76 Hz). The factor stimulus repetition significantly modulated the time-frequency representations in one region: low-frequency cluster (1–523 ms, 1–26 Hz), which was larger than the LEP cluster. In addition, a significant interaction between the two factors was found in a low-frequency cluster (141–328 ms, 1–10 Hz), indicating that the stimulus repetition reduced the strength of the relationship between intensity of perception and magnitude. Bottom left, Effect of stimulus repetition (S1–S3) at different intensities of pain (I1–I4), within the LEP and GBO regions. *x*-axis, stimulus number; *y*-axis: percentage of change relative to the reference interval (ER%). Bottom right, Effect of intensity of pain (I1–I4) at each triplet stimulus (S1–S3), within the LEP and GBO regions. *x*-axis, intensity of pain; *y*-axis: percentage of change relative to the reference interval (ER%). Error bars represent the SEM. While the activity within the LEP region was significantly modulated by both stimulus repetition (the activity following S1 was significantly greater than the activity following S2 and S3) and intensity of pain (with higher magnitudes for stimuli perceived as more intense), the activity within the GBO region was only significantly modulated by intensity of pain.

where t is the time index, a is the coefficients of the autoregressive model e_c and e_i are prediction residuals with variance σ_c and σ_i, respectively. The model order P can be selected by the Bayesian information criterion (BIC) (Schwarz, 1978).

If a smaller variance of the prediction residual of x_c (or x_i) can be achieved with the involvement of the past values of x_i (or x_c) in Equation 3 (or Equation 4), one can claim that x_i (or x_c) "Granger-causes" x_c (or x_i). The strength of Granger causality from Ci to Cc and from Cc to Ci can be respectively estimated as:

$$GC_{i\to c} = \ln(|\sigma_{c,1}|/|\sigma_{c,2}|) \quad (5)$$

$$GC_{c\to i} = \ln(|\sigma_{i,1}|/|\sigma_{i,2}|) \quad (6)$$

where $\sigma_{c,1}$ and $\sigma_{c,2}$ are, respectively, the variances of the prediction residual of x_c with and without the involvement of x_i in Equation 3. $\sigma_{i,1}$ and $\sigma_{i,2}$ are, respectively, the variances of the prediction residual of x_i with and without the involvement of x_c in Equation 4 (Geweke, 1982).

Here, the neural responses detected at Cc and Ci are summarized as the time course of ER% values within the time interval extending from 86 to 328 ms, averaged within the frequency range from 47 to 76 Hz (as specified by the GBO regions identified by the point-by-point time-frequency statistical analysis). The single-trial time courses were averaged across all epochs. Only epochs where the three stimuli elicited percepts with normalized ratings >50 were included in the analysis. The strengths of the Granger causalities from Cc to Ci and of those from Ci to Cc were then calculated for each participant and condition, and compared using a paired-sample t test.

Results

Quality and intensity of perception

For each of the four stimulus energies used (E1–E4), laser stimuli elicited a clear pinprick sensation in all participants, related to the activation of Aδ fibers (Bromm and Treede, 1984). As expected, the intensity of pain was significantly and positively correlated with the energy of the laser stimulus ($p < 0.0001$; Fig. 1). In contrast, stimulus repetition (S1–S3) did not affect the intensity of pain ($p = 0.165$; Fig. 1). Last, there was no interaction between the experimental factors stimulus energy and stimulus repetition ($p = 0.996$).

Laser-induced EEG responses

Time-frequency analysis revealed that the first laser stimulus (S1) elicited a clear phase-locked response corresponding to the LEP detected in the time-domain (LEP, 100–400 ms, 1–12 Hz) and three distinct non-phase-locked activities consisting in (1) a synchronization of beta-band EEG oscillations ("β-ERS," 100–300 ms, 12–30 Hz) followed by (2) a desynchronization of beta-band EEG oscillations ("β-ERD," 300–1000 ms, 12–25 Hz) and (3) a transient synchronization of gamma-band EEG oscillations (GBO, 100–300 ms, 30–100 Hz) (Fig. 2, top and middle). Only the LEP response showed high phase-

locking values, confirming that the other responses were indeed non-phase-locked to the stimulus onset and, hence, not detectable using conventional across-trial averaging in the time domain (Fig. 2, bottom).

Effect of stimulus repetition and intensity of pain

Figure 3 shows the average time-frequency representations classified in 12 (3 × 4) categories according to stimulus repetition (S1, S2, and S3) and intensity of pain (I1, I2, I3, and I4). The magnitude of the LEP and β-ERS responses was strongly modulated by stimulus repetition. In addition, their magnitude was positively correlated with the reported intensity of pain perception. In contrast, the magnitude of the β-ERD response was modulated neither by stimulus repetition nor by intensity of pain perception. In striking contrast with the behavior of the LEP and β-ERS responses, the magnitude of the laser-induced GBOs was not affected by stimulus repetition, but positively correlated with the reported intensity of pain perception (Fig. 3).

The two-way repeated-measures ANOVA combined with the nonparametric permutation testing identified the following significant clusters ($p < 0.001$) in the time-frequency representations of the EEG responses elicited by the laser stimuli (Fig. 4). First, the factor intensity of pain significantly modulated the signal amplitude in a low-frequency cluster (LEP: 86–367 ms, 1–16 Hz, $p < 0.001$) and a high-frequency cluster in the range of gamma-band oscillations (GBO: 86–328 ms, 47–76 Hz, $p < 0.001$). Second, the factor stimulus repetition significantly modulated the signal amplitude in a range of frequencies including both the LEP and the β-ERS response (1–523 ms, 1–26 Hz, $p < 0.001$), but, crucially, not including the GBO response. Third, there was a significant interaction between the factors stimulus repetition and intensity of pain in a low-frequency cluster (141–328 ms, 1–10 Hz, $p < 0.001$), indicating that, in this time-frequency region, stimulus repetition reduced the strength of the relationship between pain perception and signal amplitude. As the aim of this study was to characterize the laser-evoked brain responses related to the intensity of perceived pain, the signal in the two ROIs (LEP and GBO) that were both significantly modulated by the factor intensity of pain was extracted.

The summary values of the LEP cluster were significantly different at different intensities of pain perception ($F = 12.85$, $p < 0.0001$), with higher magnitudes for stimuli perceived as more intense (Table 1). *Post hoc* analyses revealed a significant linear correlation between LEP magnitude and intensity of perception ($r^2 = 0.11$, $p < 0.001$). They were also significantly different in the responses elicited by S1, S2, and S3 ($F = 34.87$, $p < 0.0001$). *Post hoc* comparisons revealed that the magnitudes of the LEP responses elicited by S2 and S3 were significantly reduced compared with the magnitude of the responses elicited by S1 ($p < 0.001$). However, the magnitude of the LEP response elicited by S2 was not significantly different from that elicited by S3 ($p = 0.16$) (Fig. 4, Table 1). The r^2 values and the slopes of the linear correlations between intensity of pain and LEP magnitude for different stimulus repetitions were as follows: S1: $r^2 = 0.22$ ($p = 0.0007$), slope = 0.99; S2: $r^2 = 0.23$ ($p = 0.0005$), slope = 0.30; S3: $r^2 = 0.32$ ($p < 0.0001$), slope = 0.33. There was also a significant interaction between the effects of stimulus repetition and intensity of pain ($F = 5.95$, $p = 0.0001$; Table 1), indicating that stimulus repetition significantly reduced the slope of the correlation between the magnitude of the LEP response and subjective pain intensity. Indeed, *post hoc* analysis revealed that the slope of the linear correlation between LEP magnitude and intensity of perception in S1 was significantly steeper than the slope of the linear correlation in S2 ($p = 0.02$) and S3 ($p = 0.01$), whereas the slopes for S2 and S3 were similar ($p = 0.62$) (Fig. 4).

In contrast, the summary values of the GBO cluster were exclusively modulated by the factor intensity of pain ($F = 6.93$, $p < 0.001$)—with higher magnitudes for stimuli perceived as more intense—and were not modulated by the factor stimulus repetition ($F = 0.15$, $p = 0.86$). Crucially, there was no interaction between the two factors ($F = 0.32$, $p = 0.92$; Tables 1 and 3)

Table 1. Two-way repeated-measures ANOVA with intensity of pain (I1–I4) and stimulus repetition (S1–S3) as factors

	LEP		GBO	
	p value	*F* value	*p* value	*F* value
ANOVA				
Intensity of pain	<0.0001***	12.85	<0.001**	6.93
Stimulus repetition	<0.0001***	34.87	0.86	0.15
Interaction	0.0001***	5.95	0.92	0.32
Post hoc t test				
Intensity of pain				
I1 versus I2	<0.001**		0.06	
I1 versus I3	<0.001**		<0.001**	
I1 versus I4	<0.001**		0.001**	
I2 versus I3	0.02*		0.006*	
I2 versus I4	0.002*		0.003*	
I3 versus I4	0.10		0.005*	
Stimulus repetition				
S1 versus S2	<0.001**		0.61	
S1 versus S3	<0.001**		0.52	
S2 versus S3	0.16		0.89	

*$p < 0.01$; **$p < 0.001$; ***$p < 0.0001$.

Table 2. Two-way repeated-measures ANOVA with stimulus energy (E1–E4) and stimulus repetition (S1–S3) as factors

	LEP		GBO	
	p value	*F* value	*p* value	*F* value
ANOVA				
Stimulus energy	0.003*	5.68	0.27	1.36
Stimulus repetition	<0.0001***	36.87	0.94	0.06
Interaction	0.009*	3.13	0.77	0.55
Post hoc t test				
Stimulus energy				
E1 versus E2	0.11		0.54	
E1 versus E3	0.003*		0.16	
E1 versus E4	0.04*		0.08	
E2 versus E3	0.009*		0.10	
E2 versus E4	0.20		0.08	
E3 versus E4	0.02*		0.51	
Stimulus repetition				
S1 versus S2	<0.001**		0.79	
S1 versus S3	<0.001**		0.61	
S2 versus S3	0.21		0.64	

*$p < 0.01$; **$p < 0.001$; ***$p < 0.0001$.

Table 3. Magnitude (ER%, expressed as mean ± SEM) of GBO elicited by S1, S2, and S3, at different intensity of pain (I1–I4)

	Stimulus repetition			
	S1	S2	S3	All stimuli
Intensity of pain				
I1	20 ± 7	18 ± 6	16 ± 6	18 ± 6
I2	27 ± 8	31 ± 9	30 ± 15	29 ± 11
I3	57 ± 22	56 ± 17	47 ± 16	53 ± 18
I4	128 ± 55	90 ± 40	98 ± 40	105 ± 45
All pain intensities	58 ± 32	49 ± 23	48 ± 24	

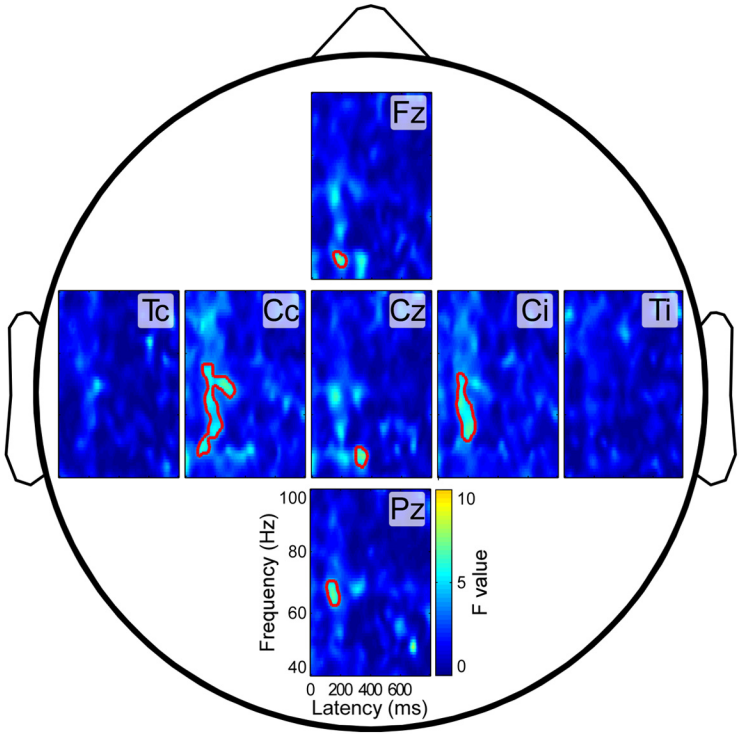

Figure 5. Scalp distribution of the main effect of intensity of pain (I1–I4) on the time-frequency representations of laser-induced modulation of EEG oscillation magnitude (ER%). *x*-axis, time (ms); *y*-axis, frequency (Hz). The color scale represents the *F*-value. The time-frequency points significantly modulated by the factor intensity of pain ($p < 0.01$, $F > 4.44$) are encircled using red lines.

indicating that stimulus repetition did not reduce the slope of the correlation between the magnitude of the GBO response and subjective pain intensity. *Post hoc* comparisons revealed a significant linear correlation between GBO magnitude and intensity of pain ($r^2 = 0.12$, $p < 0.001$). The r^2 values and the slopes of the linear correlations between intensity of pain and GBO magnitude for different stimulus repetitions were as follows: S1: $r^2 = 0.13$ ($p = 0.01$), slope = 0.34; S2: $r^2 = 0.11$ ($p = 0.02$), slope = 0.28; S3: $r^2 = 0.13$ ($p = 0.01$), slope = 0.26. The slopes of these linear correlations were not significantly different (S1 vs S2: $p = 0.61$; S1 vs S3: $p = 0.61$; S2 vs S3: $p = 0.81$), thus indicating that the magnitude of the GBO cluster was positively correlated with the intensity of perceived pain regardless of stimulus repetition, i.e., not only in the response elicited by S1, but also in the responses elicited by S2 and S3.

Figure 5 shows the scalp distribution of the *F*-values of the main effect of intensity of pain on the time-frequency representations of the laser-induced EEG responses, obtained using the two-way repeated-measures ANOVA and nonparametric permutation testing. The first and second largest significant GBO clusters were located at the contralateral and ipsilateral central electrodes (Cc and Ci), respectively.

Effect of stimulus repetition and stimulus energy

A two-way repeated-measures ANOVA combined with nonparametric permutation testing, performed with stimulus repetition (S1–S3) and stimulus energy (E1–E4) as factors, identified the following significant clusters ($p < 0.001$) in the time-frequency representations of the EEG responses elicited by the laser stimuli (Fig. 6). First, the factor stimulus energy significantly modulated the signal amplitude in a low-frequency cluster (LEP, 180–281 ms, 1–6 Hz, $p < 0.001$). Second, the factor stimulus repetition significantly modulated the signal amplitude in a large low-frequency cluster (1–797 ms, 1–26 Hz, $p < 0.001$). Third, there was a significant interaction between the two factors in a low-frequency cluster (86–227 ms, 1–18 Hz, $p < 0.001$), which indicated that, in this time-frequency region, stimulus repetition reduced the strength of the relationship between stimulus energy and signal amplitude. Notably, in contrast with the ANOVA exploring the effect of intensity of pain, no time-frequency points in the range of gamma band oscillations were significantly modulated by stimulus repetition, stimulus energy, or their interaction. As no significant cluster in the gamma range was significantly modulated by the factor stimulus energy, to quantify the effects of stimulus repetition and stimulus energy on the magnitude of laser-induced oscillations in the gamma range, the GBO clusters identified when investigating the effect of intensity of pain were used as ROIs to extract summary values.

The summary values of the LEP cluster were significantly different at different stimulus energies ($F = 5.68$, $p = 0.003$), with higher magnitudes for stimuli perceived as more intense (Table 2). *Post hoc* analyses revealed a significant linear correlation between LEP magnitude and stimulus energy ($r^2 = 0.04$, $p = 0.02$) (Fig. 6). They were also significantly different in the responses elicited by S1, S2, and S3 ($F = 36.87$, $p < 0.0001$). *Post hoc* comparisons revealed that the magnitudes of the LEP responses elicited by S2 and S3 were significantly reduced compared with the magnitude of the responses elicited by S1 ($p < 0.001$). However, the magnitude of the LEP response elicited by S2 was not significantly different from that elicited by S3 ($p = 0.21$) (Fig. 6, Table 2). The r^2 values and the slopes of the linear correlations between stimulus energy and LEP magnitude for different stimulus repetitions were as follows: S1: $r^2 = 0.14$ ($p = 0.01$), slope = 0.95; S2: $r^2 = 0.03$ ($p = 0.24$), slope = 0.18; S3: $r^2 = 0.03$ ($p = 0.22$), slope = 0.16. There was also a significant interaction between the effects of stimulus energy and stimulus repetition on the summary values of the LEP response ($F = 3.13$, $p = 0.009$) (Table 2). *Post hoc* analysis revealed that the slopes of the linear correlation between LEP magnitude and stimulus energy for S1 was significantly steeper than those for S2 ($p = 0.03$) and S3 ($p = 0.03$), whereas those for S2 and S3 were similar ($p = 0.64$) (Fig. 6). In contrast, the summary values of the GBO cluster were not significantly modulated by the factors stimulus energy ($F = 1.36$, $p = 0.27$), stimulus repetition ($F = 0.06$, $p = 0.94$) or by their interaction ($F = 0.55$, $p = 0.77$) (Table 2).

Granger causality between the GBOs recorded at contralateral and ipsilateral central electrodes

Figure 7 shows the strength and time course of the laser-induced modulation of GBOs at electrodes Cc and Ci, together with the comparison of the Granger causality indexes from Cc to Ci and from Ci to Cc. The stimulus-induced increase of GBOs at the central electrode overlying the primary somatosensory cortex contralateral to the stimulated hand causally explained the in-

crease of GBOs at the central electrodes overlying the primary somatosensory cortex ipsilateral to the stimulated hand. Indeed, the Granger causality index from Cc to Ci was significantly greater than the Granger causality index from Ci to Cc (3.22 ± 0.19 vs 2.71 ± 0.28, $p = 0.03$).

Discussion

Here we describe a neurophysiological measure that is able to predict reliably the amount of pain perception in humans, regardless of the modulation in saliency content induced by stimulus repetition. Indeed, the magnitude of the gamma band oscillations (GBO) induced in the primary somatosensory cortex by nociceptive laser stimuli repeated at short (1 s) and constant interval robustly reflected the subjective pain intensity, regardless of stimulus repetition. This finding is in striking contrast with what was observed for all other laser-evoked EEG responses, whose magnitude was strongly modulated by stimulus repetition and, hence, was not determined by the perception of pain per se, but by the saliency content of the eliciting stimulus. Although the present data do not allow concluding that these GBOs reflect cortical activity that is specific for nociception, they do provide evidence for a close relationship between GBOs and the cortical activity subserving pain perception.

Laser-induced GBOs predict subjective pain intensity independently of stimulus saliency

In striking contrast with all other EEG responses to nociceptive stimuli (Fig. 4; Iannetti et al. 2008), the magnitude of laser-induced GBOs was significantly modulated by the factor intensity of pain, independently of stimulus repetition. Indeed, stimulus repetition at a short and constant 1 s interval did not reduce the magnitude of the laser-induced GBOs, and did not disrupt the relationship between their magnitude and the subjective pain intensity. In other words, the magnitude of laser-induced GBOs was always predictive of the amount of pain perceived by the subject, and was unaffected by the novelty reduction resulting from stimulus repetition. This finding provides a major step forward in understanding the functional significance of GBOs, as it shows that they reflect cortical processes that faithfully reflect the intensity of perceived pain, regardless of the saliency content of the stimulus.

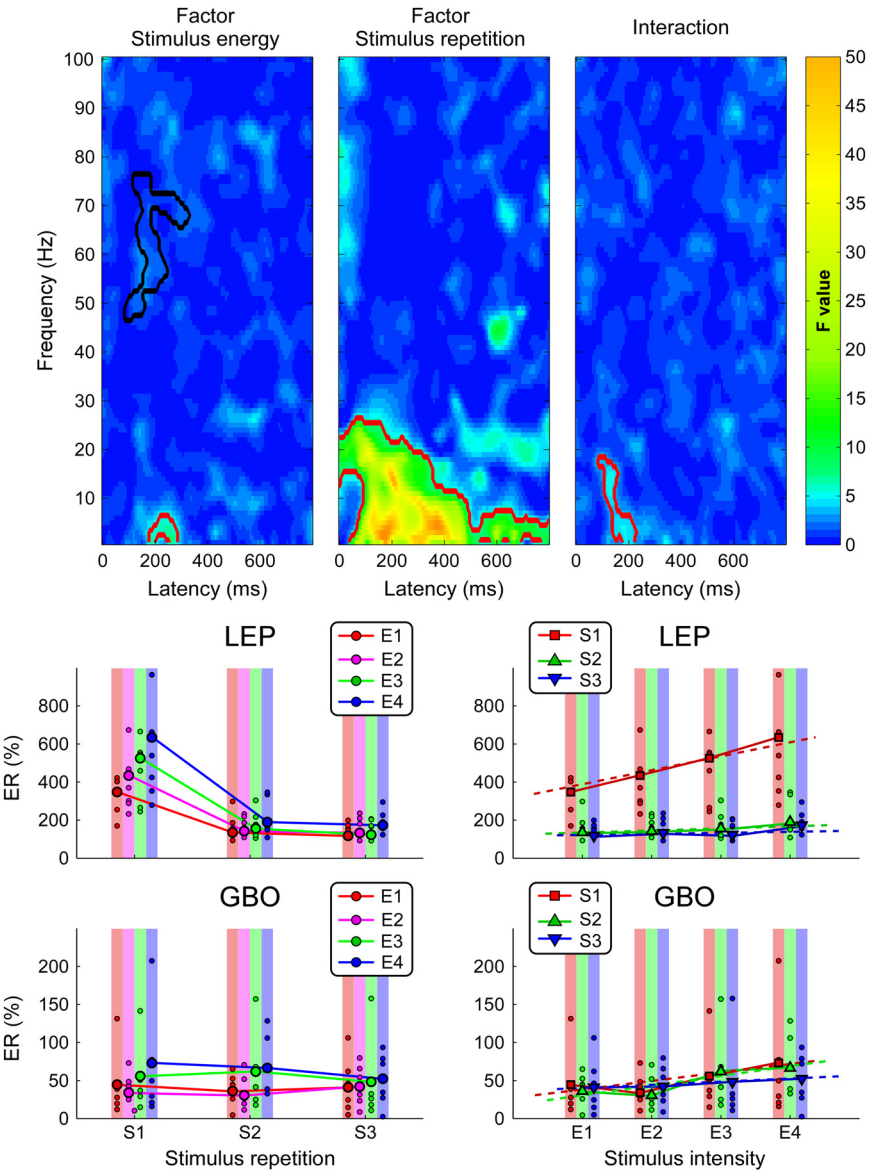

Figure 6. Effect of stimulus repetition (S1–S3) and stimulus energy (E1–E4) on the time-frequency representations of laser-induced modulation of EEG oscillation magnitude (ER%). Top, Two-way repeated-measures ANOVA to assess the effect of stimulus repetition and stimulus energy and nonparametric permutation testing to define time-frequency regions of interest. *x*-axis, time (ms); *y*-axis, frequency (Hz). The time-frequency pixels significantly affected by each experimental factor (or by the interaction between the two factors) are outlined in red. The color scale represents the *F*-values for each of the factors and their interaction. Note that the time-frequency points with $p < 0.01$ ($F > 4.44$ for the factor stimulus energy; $F > 5.72$ for the factor stimulus repetition, and $F > 5.07$ for their interaction) were selected for the subsequent nonparametric permutation testing. The factor stimulus energy significantly modulated the time-frequency representations in one region (in red): low-frequency cluster (LEP, 180–281 ms, 1–6 Hz). The factor stimulus repetition significantly modulated the time-frequency representations in one low-frequency cluster (1–797 ms, 1–26 Hz). In addition, a significant interaction between the two factors was found in a low-frequency cluster (86–227 ms, 1–18 Hz), indicating that the stimulus repetition reduced the strength of the relationship between stimulus energy and magnitude. For comparison, the GBO ROI identified in the analysis investigating the effect of stimulus repetition (S1–S3) and intensity of pain (I1–I4) on ER% (see Fig. 4) were indicated using black lines. Bottom left, Effect of stimulus repetition (S1–S3) at different stimulus energies (E1–E4), within the LEP and GBO regions. *x*-axis, stimulus number; *y*-axis: percentage of change relative to the reference interval (ER%). Bottom right, Effect of stimulus energy (E1–E4) at each triplet stimulus (S1–S3), within the LEP and GBO regions. *x*-axis, stimulus energy; *y*-axis: percentage of change relative to the reference interval (ER%). Error bars represent the SEM. Note that whereas the activity within the LEP region was significantly modulated by both stimulus repetition (the activity following S1 was significantly greater than the activity following S2 and S3) and stimulus energy (with higher magnitudes for stimuli of higher energy, but only in the response elicited by S1), the activity within the GBO region was modulated by neither stimulus repetition nor stimulus energy.

Gamma-band oscillations induced by nociceptive stimuli in SI were reported for the first time by Gross et al. (2007), using MEG. By delivering identical nociceptive laser stimuli at an energy corresponding to the threshold to elicit a painful percept, they showed that stimuli perceived as painful yielded GBOs of greater magnitude than identical stimuli not perceived as painful, concluding that laser-induced GBOs "are particularly related to

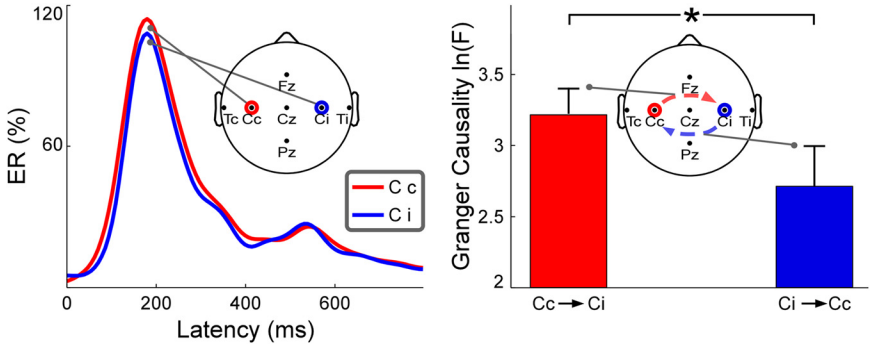

Figure 7. Strengths and causality of the laser-induced gamma oscillation magnitude at electrodes overlying the SI contralateral and ipsilateral to the stimulated hand. Left, Strength and time course of the laser-induced modulation of gamma oscillation at Cc and Ci (red and blue lines respectively). Right, Comparison of the strength of the Granger causality from Cc to Ci (in red) and from Ci to Cc (in blue). The strength of the Granger causality from Cc to Ci was significantly larger than that from Ci to Cc (3.22 ± 0.19 vs 2.71 ± 0.28, $p = 0.03$).

the subjective perception of pain" (Gross et al., 2007). However, the finding that the magnitude of the GBOs elicited by transient nociceptive stimuli delivered in isolation at long interstimulus intervals (between 10 and 14 s) correlates with the subjective pain intensity does not allow concluding that the novel responses described by Gross et al. (2007) constitute a direct correlate of pain perception. Indeed, this relationship between response magnitude and perceived pain could also result from the fact that stimuli eliciting a painful percept are necessarily more salient, i.e., more likely to capture attention, than stimuli not eliciting a painful percept. In other words, an alternative interpretation of this relationship would be that laser-induced GBOs reflect cortical activity that is unspecific for nociception, indirectly related to pain perception, and mainly related to the attentional mechanisms triggered by salient sensory input. Testing this alternative hypothesis is mandatory, considering (1) that such as the magnitude of laser-induced GBOs, the magnitude of virtually all other features of the EEG and magnetoencephalographic response also correlates with the subjective pain intensity provided that the eliciting stimuli are delivered using long and variable interstimulus intervals, but also (2) that this relationship is disrupted when the stimuli are repeated at a short and constant ISI (Bromm and Treede, 1987; Raij et al., 2003; Truini et al., 2004; Iannetti et al., 2008; for review, see Iannetti and Mouraux, 2010; Legrain et al., 2011).

The current results were obtained using a paradigm specifically designed to modulate pain perception and stimulus saliency independently, and thus to dissect the modulatory effects related to the subjective pain intensity from those related to stimulus novelty and saliency. We show that, unlike all other features of the EEG response elicited by nociceptive stimulation, the magnitude of laser-induced GBOs correlates with the amount of pain perceived, independently of stimulus saliency. This finding is of primary importance. Indeed, building upon the previous descriptions of laser-induced GBOs (Gross et al., 2007; Hauck et al., 2007; Tiemann et al., 2010; Schulz et al., 2011a,b), it demonstrates that these responses constitute a neurophysiological correlate that is related directly to the intensity of pain and, hence, are more likely to reflect activity specifically related to the processing of nociceptive input and the emergence of pain in humans. The implications of this finding are far-reaching, not only for basic research but also for clinical practice. Indeed, both diagnosis and monitoring of treatment efficacy still rely heavily on subjective and possibly biased verbal reports of pain perception (Cruccu et al., 2004; Tracey, 2011). In this respect, it will be imperative to assess the possibility of recording GBOs in a large cohort of healthy participants, not only in response to transient nociceptive stimuli but also during longer-lasting stimuli and spontaneous painful sensations, which are a hallmark of chronic pain conditions.

Neural origin and functional significance of laser-induced GBOs

Yuval-Greenberg et al. (2008) recently proposed that gamma-band oscillations induced by visual stimuli mainly originate from microsaccadic activity, thus triggering a heated debate about whether or not these responses truly reflect neural activity. The neural origin of the GBOs recorded in the present study is strongly supported by at least three lines of reasoning. First, EEG trials contaminated by eye-blinks and movements were identified and corrected using a validated ICA algorithm (Makeig et al., 1997; Jung et al., 2001; Delorme and Makeig, 2004), which has been shown to remove effectively microsaccades (Keren et al., 2010). Second, the significant GBO clusters were largest and discretely located at the contralateral and ipsilateral central electrodes (Fig. 5), suggesting that laser-induced GBOs were mainly generated in SI. This is also supported by source analysis of magnetoencephalographic data, which has provided convincing evidence that laser-induced GBOs mainly originate from SI (Gross et al., 2007; Tiemann et al., 2010). Third, Granger causality analysis revealed a clear directionality in the causal relation between the GBOs detected at the scalp sites contralateral and ipsilateral to the stimulated hand, with a clear indication that the GBOs recorded at electrodes overlying the contralateral SI determined the GBOs recorded at electrodes overlying the ipsilateral SI (Fig. 7).

There is thus converging evidence that laser-induced GBOs originate from the ipsilateral and contralateral SI. Together with the results of other recent studies (e.g., Valentini et al., 2012), this indicates a central role of SI in the processing of nociceptive stimuli. Most interestingly, the fact that GBOs constitute the only laser-induced EEG response which predicts the amount of perceived pain regardless of the saliency content of the stimulus, indicates that these neural activities originating from SI contribute directly to the emergence of a painful percept in response to nociceptive input. The early latency (86–328 ms) and short-lasting duration (242 ms) of laser-induced GBOs indicates that they are mediated by rapidly adapting type II A-fiber mechano-heat nociceptors responsible for the sensation of first pain (Treede et al., 1995). However, the possibility that GBOs reflect cortical activity that is specific for the processing of somatosensory input, but not specific for the processing of nociceptive input should not be dismissed. Indeed, several studies have shown that non-nociceptive somatosensory stimuli also elicit GBOs within SI (Chen and Herrmann, 2001; Bauer et al., 2006; Fukuda et al., 2008). Hence, nociceptive and non-nociceptive somatosensory GBOs could reflect similar cortical responses, involved in the initial selection and preferential processing of somatosensory stimuli regardless of whether they are nociceptive. Since GBOs have been shown to underlie the synchronization of not only local, but also distant neuronal groups, the finding of discrete and causally related GBOs at contralateral and ipsilateral central electrodes strongly suggests that observed somatosensory GBOs underlie an early transmission of somatosensory input from the contralateral to the ipsilateral SI (Fig. 7).

We observed that the magnitude of laser-induced GBOs correlates significantly with the subjective pain intensity, but not with the actual stimulus energy (Tables 1, 2; Figs. 4, 6). This dissociation could be explained entirely by a combination of peripheral factors (e.g., fluctuations in skin temperature, variability in density, threshold and conduction velocity of type II AMH nociceptors) resulting in a significant difference between the energy of the laser pulse, and the

strength of the elicited afferent input in peripheral nociceptors. However, it could also be explained by variability in the central processing of the nociceptive afferent input, resulting from fluctuations in vigilance, focus of attention or task strategy (Legrain et al., 2002, 2003; Lee et al., 2009), as well as by the limited number of participants of the present study. Nevertheless, the finding that the magnitude of laser-induced GBOs is more closely related to pain perception than to the actual energy of the nociceptive stimulus, together with the large body of evidence indicating that oscillatory activity in the gamma range constitutes a mechanism for integrating low-level cortical processing of basic stimulus features with higher-order cognitive processes like attention and anticipation (Hauck et al., 2007; Tiemann et al., 2010), suggest that laser-induced GBOs represent cortical activity lying at the very interface between stimulus-driven and top-down determinants of the perception of pain.

References

Astolfi L, Bakardjian H, Cincotti F, Mattia D, Marciani MG, De Vico Fallani F, Colosimo A, Salinari S, Miwakeichi F, Yamaguchi Y, Martinez P, Cichocki A, Tocci A, Babiloni F (2007) Estimate of causality between independent cortical spatial patterns during movement volition in spinal cord injured patients. Brain Topogr 19:107–123.

Bauer M, Oostenveld R, Peeters M, Fries P (2006) Tactile spatial attention enhances gamma-band activity in somatosensory cortex and reduces low-frequency activity in parieto-occipital areas. J Neurosci 26:490–501.

Baumgärtner U, Cruccu G, Iannetti GD, Treede RD (2005) Laser guns and hot plates. Pain 116:1–3.

Bromm B, Treede RD (1984) Nerve fibre discharges, cerebral potentials and sensations induced by CO2 laser stimulation. Hum Neurobiol 3:33–40.

Bromm B, Treede RD (1987) Human cerebral potentials evoked by CO2 laser stimuli causing pain. Exp Brain Res 67:153–162.

Chen AC, Herrmann CS (2001) Perception of pain coincides with the spatial expansion of electroencephalographic dynamics in human subjects. Neurosci Lett 297:183–186.

Cruccu G, Anand P, Attal N, Garcia-Larrea L, Haanpää M, Jørum E, Serra J, Jensen TS (2004) EFNS guidelines on neuropathic pain assessment. Eur J Neurol 11:153–162.

Delorme A, Makeig S (2004) EEGLAB: an open source toolbox for analysis of single-trial EEG dynamics including independent component analysis. J Neurosci Methods 134:9–21.

Downar J, Crawley AP, Mikulis DJ, Davis KD (2000) A multimodal cortical network for the detection of changes in the sensory environment. Nat Neurosci 3:277–283.

Fries P (2009) Neuronal gamma-band synchronization as a fundamental process in cortical computation. Annu Rev Neurosci 32:209–224.

Fukuda M, Nishida M, Juhász C, Muzik O, Sood S, Chugani HT, Asano E (2008) Short-latency median-nerve somatosensory-evoked potentials and induced gamma-oscillations in humans. Brain 131:1793–1805.

Geweke J (1982) Measurement of linear dependence and feedback between multiple time series. J Am Stat Assoc 77:304–313.

Granger CWJ (1969) Investigating causal relations by econometric models and cross-spectral methods. Econometrica 37:424–438.

Gross J, Schnitzler A, Timmermann L, Ploner M (2007) Gamma oscillations in human primary somatosensory cortex reflect pain perception. PLoS Biol 5:e133.

Hauck M, Lorenz J, Engel AK (2007) Attention to painful stimulation enhances gamma-band activity and synchronization in human sensorimotor cortex. J Neurosci 27:9270–9277.

Herrmann CS, Kaiser J (2011) EEG gamma-band responses reflect human behavior: an overview. Int J Psychophysiol 79:1–2.

Iannetti GD, Mouraux A (2010) From the neuromatrix to the pain matrix (and back). Exp Brain Res 205:1–12.

Iannetti GD, Zambreanu L, Tracey I (2006) Similar nociceptive afferents mediate psychophysical and electrophysiological responses to heat stimulation of glabrous and hairy skin in humans. J Physiol 577:235–248.

Iannetti GD, Hughes NP, Lee MC, Mouraux A (2008) Determinants of laser-evoked EEG responses: pain perception or stimulus saliency? J Neurophysiol 100:815–828.

Jensen MP, Karoly P (2001) Self-report scales and procedures for assessing pain in adults. In: Handbook of pain assessment (Turk DC, Melzack R, eds), pp 15–34. New York: Guilford.

Jung TP, Makeig S, Westerfield M, Townsend J, Courchesne E, Sejnowski TJ (2001) Analysis and visualization of single-trial event-related potentials. Hum Brain Mapp 14:166–185.

Karns CM, Knight RT (2009) Intermodal auditory, visual, and tactile attention modulates early stages of neural processing. J Cogn Neurosci 21:669–683.

Keren AS, Yuval-Greenberg S, Deouell LY (2010) Saccadic spike potentials in gamma-band EEG: characterization, detection and suppression. Neuroimage 49:2248–2263.

Lachaux JP, Rodriguez E, Martinerie J, Varela FJ (1999) Measuring phase synchrony in brain signals. Hum Brain Mapp 8:194–208.

Lee MC, Mouraux A, Iannetti GD (2009) Characterizing the cortical activity through which pain emerges from nociception. J Neurosci 29:7909–7916.

Legrain V, Guérit JM, Bruyer R, Plaghki L (2002) Attentional modulation of the nociceptive processing into the human brain: selective spatial attention, probability of stimulus occurrence, and target detection effects on laser evoked potentials. Pain 99:21–39.

Legrain V, Bruyer R, Guérit JM, Plaghki L (2003) Nociceptive processing in the human brain of infrequent task-relevant and task-irrelevant noxious stimuli. A study with event-related potentials evoked by CO2 laser radiant heat stimuli. Pain 103:237–248.

Legrain V, Iannetti GD, Plaghki L, Mouraux A (2011) The pain matrix reloaded: a salience detection system for the body. Prog Neurobiol 93:111–124.

Makeig S, Jung TP, Bell AJ, Ghahremani D, Sejnowski TJ (1997) Blind separation of auditory event-related brain responses into independent components. Proc Natl Acad Sci U S A 94:10979–10984.

Maris E, Oostenveld R (2007) Nonparametric statistical testing of EEG- and MEG-data. J Neurosci Methods 164:177–190.

Mouraux A, Iannetti GD (2008) Across-trial averaging of event-related EEG responses and beyond. Magn Reson Imaging 26:1041–1054.

Ploner M, Schoffelen JM, Schnitzler A, Gross J (2009) Functional integration within the human pain system as revealed by Granger causality. Hum Brain Mapp 30:4025–4032.

Raij TT, Vartiainen NV, Jousmäki V, Hari R (2003) Effects of interstimulus interval on cortical responses to painful laser stimulation. J Clin Neurophysiol 20:73–79.

Rodriguez E, George N, Lachaux JP, Martinerie J, Renault B, Varela FJ (1999) Perception's shadow: long-distance synchronization of human brain activity. Nature 397:430–433.

Sato JR, Takahashi DY, Arcuri SM, Sameshima K, Morettin PA, Baccalá LA (2009) Frequency domain connectivity identification: an application of partial directed coherence in fMRI. Hum Brain Mapp 30:452–461.

Schoffelen JM, Gross J (2009) Source connectivity analysis with MEG and EEG. Hum Brain Mapp 30:1857–1865.

Schulz E, Zherdin A, Tiemann L, Plant C, Ploner M (2011a) Decoding an individual's sensitivity to pain from the multivariate analysis of EEG data. Cereb Cortex. Advance online publication. Retrieved July 17, 2011. doi:10.1093/cercor/bhr186.

Schulz E, Tiemann L, Schuster T, Gross J, Ploner M (2011b) Neurophysiological coding of traits and states in the perception of pain. Cereb Cortex 21:2408–2414.

Schwarz G (1978) Estimating dimension of a model. Ann Stat 6:461–464.

Tallon-Baudry C, Bertrand O, Delpuech C, Permier J (1997) Oscillatory gamma-band (30–70 Hz) activity induced by a visual search task in humans. J Neurosci 17:722–734.

Tiemann L, Schulz E, Gross J, Ploner M (2010) Gamma oscillations as a neuronal correlate of the attentional effects of pain. Pain 150:302–308.

Tracey I (2011) Can neuroimaging studies identify pain endophenotypes in humans? Nat Rev Neurol 7:173–181.

Treede RD, Meyer RA, Raja SN, Campbell JN (1995) Evidence for two different heat transduction mechanisms in nociceptive primary afferents innervating monkey skin. J Physiol 483:747–758.

Truini A, Rossi P, Galeotti F, Romaniello A, Virtuoso M, De Lena C, Leandri M, Cruccu G (2004) Excitability of the Adelta nociceptive pathways as assessed by the recovery cycle of laser evoked potentials in humans. Exp Brain Res 155:120–123.

Valentini E, Hu L, Chakrabarti B, Hu Y, Aglioti SM, Iannetti GD (2012) The primary somatosensory cortex largely contributes to the early part of the cortical response elicited by nociceptive stimuli. Neuroimage 59:1571–1581.

Womelsdorf T, Fries P, Mitra PP, Desimone R (2006) Gamma-band synchronization in visual cortex predicts speed of change detection. Nature 439:733–736.

Yuval-Greenberg S, Tomer O, Keren AS, Nelken I, Deouell LY (2008) Transient induced gamma-band response in EEG as a manifestation of miniature saccades. Neuron 58:429–441.